MR Damper Structural Control Using a Multi-Level Sliding Mode Controller

N. M. Kwok, T. H. Nguyen, Q. P. Ha, J. Li and B. Samali

Faculty of Engineering
University of Technology, Sydney
Broadway, NSW 2007, Australia

ABSTRACT

Magnetorheological (MR) fluid dampers have been an attractive candidate in structural control because of its great potential in the mitigation of dynamic effects caused by seismic excitations in civil engineering structures. The MR damper features a passive mode that is fault-safe under disastrous situations such as earthquakes. It also requires only a very small amount of driving power as compared to the active mass control devices. A major drawback of MR damper applications is, however, the nonlinear hysteresis characteristics in the force/velocity relationship. Sliding mode control, well-recognised for its super-property of robustness to parametric uncertainties and un-modelled disturbances in control systems, appears to be suitable for structural control using MR dampers. To overcome the difficulty in obtaining an exact parameter set characterising the MR damper dynamics in a wide operating range, the effect of uncertainties arisen from the damper parameters is to be handled by using a multi-level sliding mode controller, proposed in this paper. Here, the control effort is quantised into a finite number of levels, corresponding to an appropriate set of the damper parameters. This approach avoids the need for extensive parameter identification experiments, and also the unnecessary energy consumption usually associated with the discontinuous control component. The effectiveness of the proposed controller is demonstrated by simulations.

1. INTRODUCTION

As human society develops, civil structures are being built at an enormous pace. It becomes, therefore, a crucial requirement to protect the structures against adverse conditions, e.g., earthquakes, so that lives of human occupants can be safeguarded. A possible approach is to fabricate strong structures but this inevitably incurs a high capital cost. Alternatives are developed from the adoption of active and semi-active control techniques (Spencer and Sain 1997, Nishitani and Inoue 2001).

Among the active control methods, a mass is usually installed on the top of the building and its movement is controlled such that responses of the building to excitations are reduced (Adhikari and Yamaguchi 1997, Ikeda *et al*. 2001, Ha *et al*. 2001). A major disadvantage of these methods is that a power source is needed to implement the control action while this power source itself may not be available during hazardous situations. Hybridisation of active and passive control also finds its application in base isolations (Zhao *et al*. 2000) where the demand for power sources at critical moments is partly relaxed.

On the other end of the structural control spectrum, one may find a promising application of such device as the magnetorheological fluid damper (MR damper) being well applicable. Semi-active in nature, this device is able to change its damping force upon the application of an external magnetic field (Alvarez and Jimenez 2003). The salient advantage of this device is that it can be operated in a passive mode when acting as a conventional mechanical damper. Another advantage is that the power required is comparatively small and can therefore remain in operation during an earthquake (see, e.g. Spencer *et al*. 1996 and Djajakesukma *et al*. 2002). Although the MR damper is so attractive, it inherits a major weakness from its non-linear hysteretic force/velocity characteristics. Consequently, complicated modelling and parameter identification are required before the damper can be put into successful control applications.

In implementing MR damper based structural control, neural networks have been employed in modelling the damper (Wang and Liao 2005). The neural network is also applied in active control of structures under earthquake excitation (Cho *et al*. 2005). Other control techniques that have been applied in various research publications include the adaptive bang-bang control (Lim *et al*. 2003) and sliding mode fuzzy control (Kim and Yun 2000). Although applied in some control domains, fuzzy control design normally requires some form of empirical expertise or the use of some tuning schemes (Wang and Lee 2002).

For high performance, robust techniques are suggested for the area of structural control. Several control strategies were compared in (Jansen and Dyke 2000). Among these control strategies, namely, the Lyapunov design, decentralised bang-bang, maximum energy dissipation and clipped-optimal control; the clipped-optimal control was found to outperform the others. This kind of control strategy can be cast in the category of switching control where the variable structure or sliding mode control (Edwards and Spurgeon 1998) has demonstrated successful applications to non-linear and uncertain systems (Lu and Zhao 2001). In particular, promising structural control results have been reported in (Yang *et al*. 1994).

The related work previously cited prompt to the suggestion that a sliding mode controller is effective in reducing seismic excitations in structures. The MR damper also has another attractive feature in building control because of its fault-safe passive operation mode. In this work, the MR damper is employed in reducing earthquake excitations of a 5-storey scaled down building (Djajakesukma *et al*. 2002). In order to cope with the non-linear hysteresis force/velocity characteristic, a sliding mode controller (SMC) is proposed. As a too complicated model for a MR damper, obtained via any identification technique, may not be necessarily required for the control purpose. The modelling uncertainties can be handled by the SMC for its proven robust performance. Furthermore, the control force is quantised such that a limited damper parameter identification tests becomes sufficient with moderate energy consumption by the discontinuous control.

The rest of the paper is organised as follows. A system description of the building structure under control is given in Section 2. The quantised sliding mode approach is developed in Section 3. In Section 4, simulation results are included to demonstrate the effectiveness of the proposed approach. Finally, a conclusion is drawn in Section 5.

2. SYSTEM DESCRIPTION

Consider the structure of a 5-storey building model as shown in Fig. 1. The MR damper is mounted on a fixture on the ground and connected to the first floor. Each floor has lumped parameters of mass m_i, damping c_i and stiffness k_i (i=1…5) respectively. The displacement of each floor, x_i, with respect to the ground is denoted as

$$\mathbf{x} = [x_1\ x_2\ x_3\ x_4\ x_5]^T , \qquad (1)$$

where superscript (T) stands for vector or matrix transpose. The ground is assumed to be excited by an external vibration source, e.g., earthquake, in the horizontal direction given by acceleration $\ddot{x}_0$.

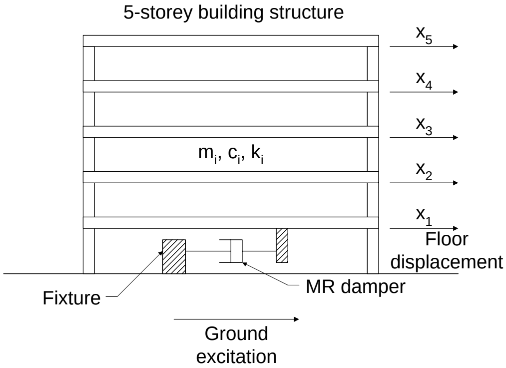

Fig. 1. 5-storey building structure under control.

The equation of motion can be written as

$$\mathbf{M}\ddot{\mathbf{x}} + \mathbf{C}\dot{\mathbf{x}} + \mathbf{K}\mathbf{x} = \mathbf{\Gamma} f + \mathbf{M}\mathbf{\Lambda}\ddot{x}_0 , \qquad (2)$$

where **M** is the mass matrix, **C** is the damping matrix and **K** is the stiffness matrix for dimension 5-by-5, $\mathbf{\Gamma}$ is the damper location vector, f is the MR damper force and $\mathbf{\Lambda}$ is the excitation distribution vector.

One can further re-write the equation of motion in the state-space form as

$$\dot{\mathbf{z}} = \mathbf{A}\mathbf{z} + \mathbf{B}f + \mathbf{E}\ddot{x}_0 , \qquad (3)$$

where $\mathbf{z}$ is the stacked state vector, **A, B** and **E** are the system, gain matrix and disturbance matrices respectively and are expressed below as

$$\mathbf{z}=\begin{bmatrix}\mathbf{x}\\ \dot{\mathbf{x}}\end{bmatrix}, \mathbf{A}=\begin{bmatrix}\mathbf{0} & \mathbf{I}\\ -\mathbf{M}^{-1}\mathbf{K} & -\mathbf{M}^{-1}\mathbf{C}\end{bmatrix}, \mathbf{B}=\begin{bmatrix}\mathbf{0}\\ \mathbf{M}^{-1}\Gamma\end{bmatrix}, \mathbf{E}=\begin{bmatrix}\mathbf{0}\\ \boldsymbol{\Lambda}\end{bmatrix}, \boldsymbol{\Gamma}=\begin{bmatrix}1\\0\\0\\0\\0\end{bmatrix}, \boldsymbol{\Lambda}=\begin{bmatrix}1\\1\\1\\1\\1\end{bmatrix}, \quad (4)$$

$$\mathbf{M}=\begin{bmatrix}m_1 & & & & \\ & m_2 & & \mathbf{0} & \\ & & m_3 & & \\ & \mathbf{0} & & m_4 & \\ & & & & m_5\end{bmatrix}, \mathbf{C}=\begin{bmatrix}c_1+c_2 & -c_2 & & & \mathbf{0}\\ -c_2 & c_2+c_3 & -c_3 & & \\ & -c_3 & c_3+c_4 & -c_4 & \\ & & -c_4 & c_4+c_5 & -c_5\\ \mathbf{0} & & & -c_5 & c_5\end{bmatrix}, \mathbf{K}=\begin{bmatrix}k_1+k_2 & -k_2 & & & \mathbf{0}\\ -k_2 & k_2+k_3 & -k_3 & & \\ & -k_3 & k_3+k_4 & -k_4 & \\ & & -k_4 & k_4+k_5 & -k_5\\ \mathbf{0} & & & -k_5 & k_5\end{bmatrix}. \quad (5)$$

The control objective is to reduce the displacements and mitigate vibrational effects due to an earthquake excitation.

3. SLIDING MODE CONTROL

Sliding mode control (SMC) is a robust control technique designed for systems subject to model uncertainties and external disturbances (Edwards and Spurgeon 1998). Within the SMC framework, a nominal system is formulated while all uncertainties and disturbances are excluded from the system. A *sliding surface* is designed such that the system response along the sliding surface

$$\sigma = \mathbf{S}\mathbf{z} = 0 \quad (6)$$

is stable and satisfies some performance criteria determined by the sliding matrix **S**.

The SMC output **u** consists of two components, namely, an equivalent control $\mathbf{u_e}$ and a switching control $\mathbf{u_s}$. That is

$$\mathbf{u} = \mathbf{u_e} + \mathbf{u_s}\ , \quad (7)$$

where $\mathbf{u_e}$ is responsible for ensuring the system state to remain on the sliding surface (sliding phase or mode) and $\mathbf{u_s}$ for compensating uncertainties and disturbances such that the system state is driven towards the sliding surface (reaching phase).

There are various methods in designing the equivalent control, for example, linear quadratic regulator (LQR), pole placement and others. In this work, we choose the LQR design for its satisfactory performances in most structural control systems found in practice. A cost function is firstly defined as

$$\mathbf{J} = \int \mathbf{z}^T \mathbf{Q}\mathbf{z}dt\ . \quad (8)$$

Here the cost matrix **Q** is chosen as

$$\mathbf{Q} = \mathbf{diag}(100\ 100\ 100\ 100\ 100\ 1\ 1\ 1\ 1\ 1)\ , \quad (9)$$

giving equivalent stable system poles at

$$(-0.156\pm1.70\mathrm{i}, -0.19\pm1.26\mathrm{i}, -0.23\pm0.81\mathrm{i}, -0.11\pm0.29\mathrm{i}, -0.10,\ -0.40)\times10^2\ . \quad (10)$$

In the complex plane and the LQR gain obtained as

$$\mathbf{F} = [1.59, -5.61, 4.81, -1.86, 0.47, 0.06, -0.03, 0.00, 0.00, 0.00]\times10^6\ . \quad (11)$$

The equivalent control is then given by

$$\mathbf{u_e} = -\mathbf{F}\mathbf{z}\ . \quad (12)$$

Following the development in (Edwards and Spurgeon 1998), the switching control can be designed via the application of the Lyapunov stability theorem where the candidate Lyapunov function is

$$V = \frac{1}{2}\sigma^2\ . \quad (13)$$

In the sliding mode, it requires that

$$\dot{V} = \sigma\dot{\sigma} = 0 \text{ for } \sigma = 0 . \tag{14}$$

That is

$$\dot{V} = \sigma\mathbf{S}\dot{\mathbf{z}} = \sigma\mathbf{S}(\mathbf{Az} + \mathbf{Bu}) = \sigma(\mathbf{SAz} + \mathbf{SBu}) = 0. \tag{15}$$

An equivalent control can be then obtained as

$$\mathbf{u_e} = -(\mathbf{SB})^{-1}\mathbf{SAz} . \tag{16}$$

If the response on the sliding surface is designed from the LQR approach, then the feedback gain in (11) can be obtained as

$$\mathbf{F} = (\mathbf{SB})^{-1}\mathbf{SA} , \tag{17}$$

from which the sliding matrix **S** can be derived (Ha *et al*., 2003).

Using the calculated LQR gain **F**, the sliding matrix is obtained as

$$\mathbf{S} = [-142.25 \ 139.52 \ -15.69 \ 2.95 \ -2.44 \ -1.00 \ -1.16 \ 0.11 \ -0.36 \ -0.26] . \tag{18}$$

Furthermore, the reaching condition requires that

$$\dot{V} = \sigma\dot{\sigma} < 0 \text{ for } \sigma \neq 0 . \tag{19}$$

With the derived equivalent control, we have

$$\dot{V} = \sigma\mathbf{SBu_s} < 0 . \tag{20}$$

One may choose the switching control as

$$\mathbf{u_s} = -\eta(\mathbf{SB})^{-1} sign(\sigma) \tag{21}$$

where $\eta > 0$ is determined by the bound on the disturbance and *sign* is the signum function.

The system structure including the MR damper-building model and the controller is depicted in Fig. 2.

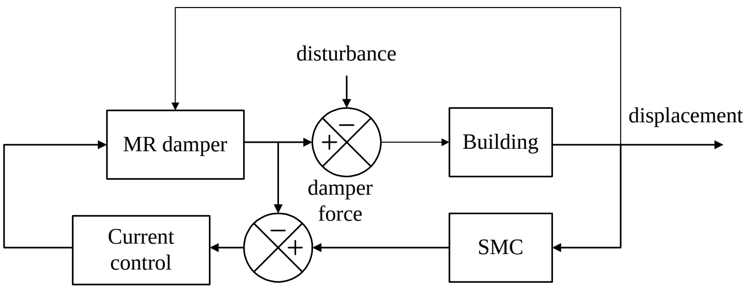

Fig. 2. System structure.

The MR damper is characterised by the widely adopted Bouc-Wen model for its relative small hysteresis approximation error and a small set of parameters. The damper force (which is **u** in the control law (7)) is given by

$$\begin{aligned} f &= c_o\dot{x} + k_0(x - x_0) + \alpha z \\ \dot{z} &= \delta\dot{x} - \beta\dot{x}\,|z|^n - \gamma z\,|\dot{x}||z|^{n-1}, \end{aligned} \tag{22}$$

where $c_0, k_0, x_0, \alpha, \delta, \beta, \gamma,$ and n are the damper parameters identified in an off-line routine.

However, the MR damper capacity is always limited in practice, $|f| \leq F_{\max}$, or an exact damping force cannot be produced due to actuator uncertainties. In this work, the damping force produced by the MR damper is assumed to be physically limited. Moreover, damper parameters are difficult to be identified over the complete operation range. From the control energy point of view, it is on one hand not necessary to apply the full magnitude of the switching control (determined by η in (21)). On the other hand, by the fact that the disturbance rejection level is limited with a given actuator capacity, it is also not necessary to apply full actuator capacity at small values of the equivalent control, otherwise the extra actuation may give rise to chattering as commonly encountered in SMC. This gives a rationale for our proposed multi-level sliding mode control approach, described as below.

The control force output from the SMC (in equ. (7)) is further processed into quantised levels according to the following rule,

$$\begin{array}{l} \text{if } f > 0 \\ \quad \text{if } f > \text{Fmax}/2 \text{ then } f = \text{Fmax} \\ \quad \text{else } f = \text{Fmax}/2 \\ \text{else} \\ \quad \text{if } f < \text{-Fmax}/2 \text{ then } f = \text{-Fmax} \\ \quad \text{else } f = \text{-Fmax}/2, \end{array} \qquad (23)$$

where Fmax is the maximum damper capacity. A typical trace of the control force is depicted in Fig. 3.

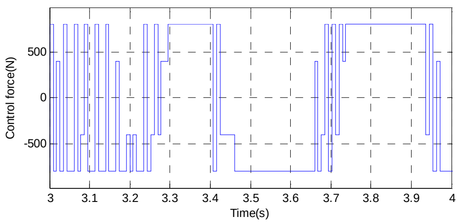

Fig. 3. Typical quantised control force.

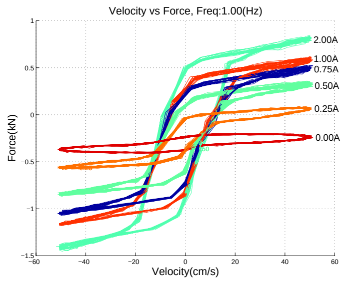

Fig. 4. Typical MR damper hysteresis

From the sketch of typical MR damper hysteresis characteristic shown in Fig. 4, and given the measured displacement and velocity of the first floor, a table-lookup procedure is implemented to determine the required current supply to the damper.

4. SIMULATION

The developed controller is applied to the control of the 5-storey model building installed at the University of Technology, Sydney. The model structure is a metal frame with add-on weights to emulate the mass of the floors and the damping and stiffness parameters are identified from a separate work (Djajakesukma *et al*. 2002). The structure has a fundamental natural frequency of about 2.5Hz. A scaled down El-Centro earthquake record, see Fig. 5, is used as the external disturbance or excitation. The parameters for the building are given in the Appendix.

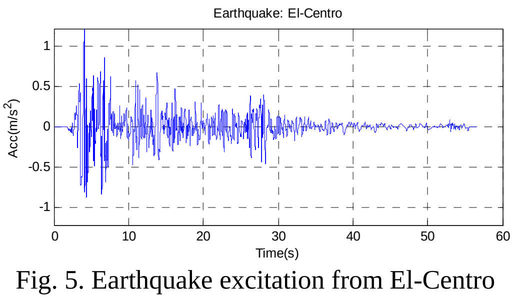

Fig. 5. Earthquake excitation from El-Centro earthquake record (scaled down).

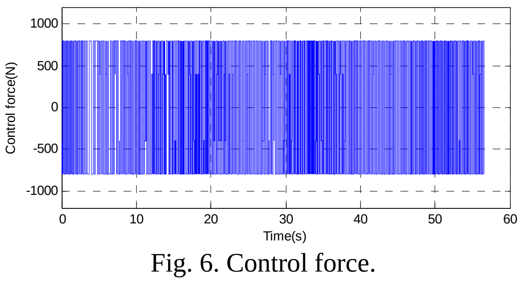

Fig. 6. Control force.

Two cases were simulated. Case 1 is the free-running response of the building to earthquake and the displacements of each floor are recorded (dotted lines). The application of the proposed controller is used in Case 2 with the design parameters presented in Section 3. The control force output from the controller is shown in Fig. 6. The displacement results are shown in Fig. 7(a) through 7(e) for the 1st floor to 5th floor (solid lines). It is illustrated that a significant reduction in earthquake response is achieved. Earthquake records from Hachinohe, Kobe and Northridge were also used in simulation. Maximum and RMS displacements are tabulated in Table 1. All results show unanimously a significant reduction in earthquake responses.